MEASUREMENT-BASED DESCRIPTION OF THE TEMPERATURE DISTRIBUTION IN LARGE ATMOSPHERIC HEAT STORAGE TANKS

Luise Umbreit, Andreas Herwig and Karin Rühling
Institute of Power Engineering, Professorship of Building Energy Systems and Heat Supply,
Technische Universität Dresden, Dresden, 01062, Germany, +49-351 / 463-32971,
Luise.Umbreit@tu-dresden.de

Abstract – The presented research project uses an innovative measurement technology to investigate large atmospheric heat storage tanks which are operated with water as storage medium. There is already sound knowledge about heat storage systems at small scales as used in single buildings in literature and software engineering as well. On the other hand, for large atmospheric heat storage tanks there are only a few scientific descriptions in literature and simulation models available. The measurement data combined with simulation results are used to gain further insight into load management in district heating especially with respect to increasing levels of renewable based feed-in. In this publication, the focus is set on particular aspects concerning the physics of one-zone and two-zone atmospheric heat storage tanks.

1. MEASUREMENT TECHNOLOGY

In order to investigate their physical behaviour under real operation conditions four one-zone and two two-zone heat storage tanks at scales between 2,000 m³ and 43,000 m³ had been equipped with a distributed temperature sensing (DTS) measurement system. The DTS-measurement principle (Figure 1) is based on the RAMAN-effect to gain precise information about the temperature distribution both in space and in time along one single glass fibre cable (Smolen and van der Spek, 2003). The measurement data had been used to create animated visualizations that depict the operation mode of the heat storage tanks in general (Rühling et. al., 2016). Due to realizing an adapted measurement concept for each monitoring and developing appropriate analysis algorithms more detailed information can be revealed. Hence, different physical effects on thermal stratification within heat storage tanks can be proven. This paper presents some subset results for both researched types of heat storage tanks.

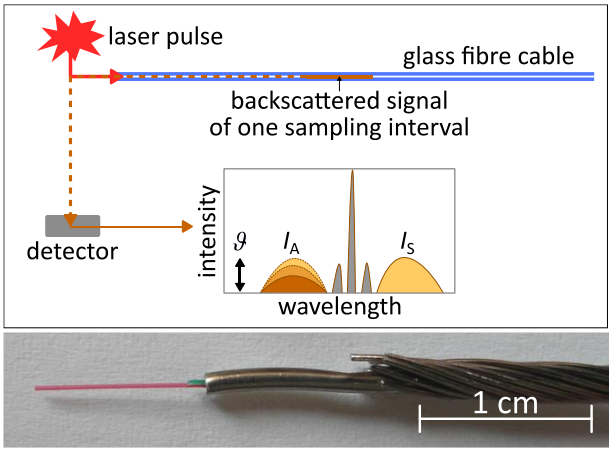

Figure 1: Top: Scheme of the DTS-measurement system. Corresponding to the RAMAN-effect, the frequency-shifted backscattering signal of a laser pulse running through a glass fibre cable features two components: The Stokes signal I_S and the Anti-Stokes signal I_A The space- and time-resolved temperature ϑ of the fibre can be determined from the detected intensity ratio of both components.
Bottom: Structure of the stainless steel sheathed glass fibre cable installed in the heat storage tanks.

2. ATMOSPHERIC ONE-ZONE HEAT STORAGE TANKS

2.1 General physics and operating mode

A common and widely realized type of large atmospheric heat storage tanks is based on the design of HEDBÄCK. They are built as pressure-less standing cylinders with one radial diffuser at the bottom and one at the top of the storage volume. During the charge process, warm water is entering the tank through the top radial diffuser and cold water is leaving through the bottom radial diffuser. While discharging the heat storage tank the flow is directed reversely. As both radial diffusers are concentric with the cylindrical storage tank they induce a radial free jet (Figure 2). In most cases the charging and discharging temperatures are well defined, hence a thermal stratification with a layer of high temperature above one layer of lower temperature is formed, with a thermocline in between. This heat storage tank design is optimized for capacities of up to several 10,000 m³ of water. More than 100 of these heat storage tanks had been built during the past decades.

The grade of stratification inside the heat storage tank limits the amount of heat which can be discharged at the required supply temperature level. Therefore a good understanding of the main factors that have an impact on the stratification is important for both: to give advice to the operation management and to generate valid models of this type of heat storage tank.

Main influences on the thermal stratification within the heat storage tank had been mentioned in (Herwig and Rühling, 2014).

2.2 Measurement concept

The measurement concept includes the DTS-measurement system and additional operating data of the heat storage tank as well. As shown in Figure 2 the DTS system captures the temperature field vertically at four radial and two additional circumferential positions: R1, R2, R3=U3, R4 and U1 and U2. Supplementary operating data is available for 19 vertically aligned PT100 temperature sensors, supply and return temperatures, volume flow and pressure at the bottom of the heat storage tank.

The temperature resolution is limited by random noise that can be reduced by averaging consecutive measurements. However, time resolution must be considered carefully. The presented work uses an average time of one minute. For this mean type the conditions inside the heat storage tank are assumed as sufficiently constant. As the focus is set on radial homogeneity of the temperature field in this study, temperature differences are formed at the same height between the six vertical positions. By the use of one-minute averages the DTS-system achieves a resolution, defined by the 1-σ standard deviation, of about 0.1 K for the radial temperature differences. The spatial resolution along the cable is 0.35 m.

By a step of calibration, the mean temperature of vertical measuring points is optimised to eleiminate small perturbations of the DTS system. Consequently, the measured temperature profiles can be compared only in terms of their shape, but not in terms of their absolute position. Since the corrections are only in the range of a few hundredths of a K, this aspect should not be discussed further in the following.

2.3 Radial homogeneity of the temperature field

The radial homogeneity of the temperature field is investigated based at the four positions R1 to R4. The position R3 represents the reference section which is used to compare the temperatures obtained at the other positions.

In Figure 3 solid lines on the right side represent the temperatures at the four radial positions during a standstill phase of the highly charged heat storage tank. Dashed lines on the left side related to the scale at the x2 axis indicate the temperature differences to R3 in each case. The gray lines marked with D indicate the position of the two diffusers. The temperature differences to R3 occurring in Figure 3 remain at very small scales over the entire height of the heat storage tank and are caused by the random noise

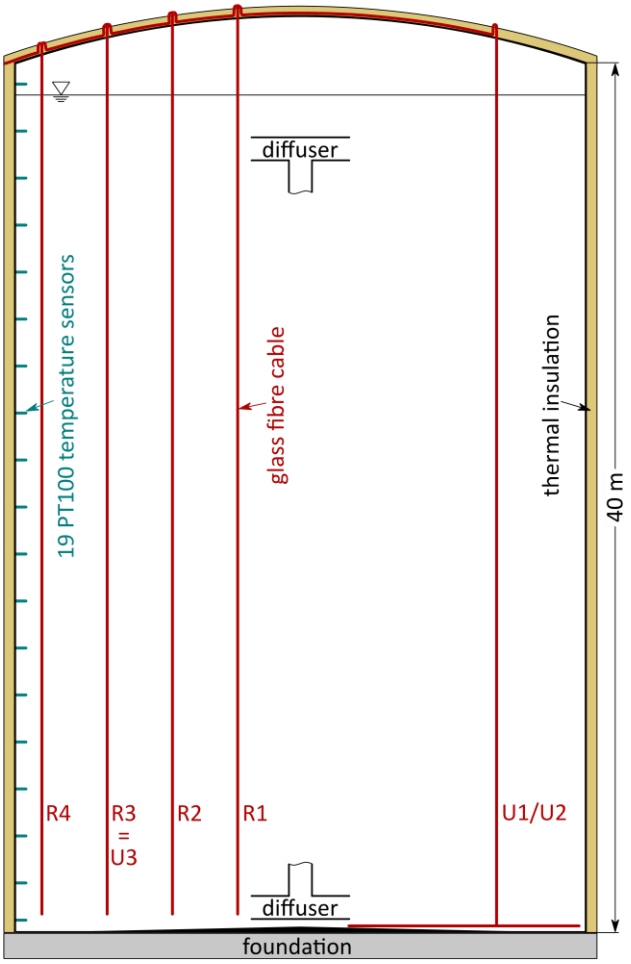

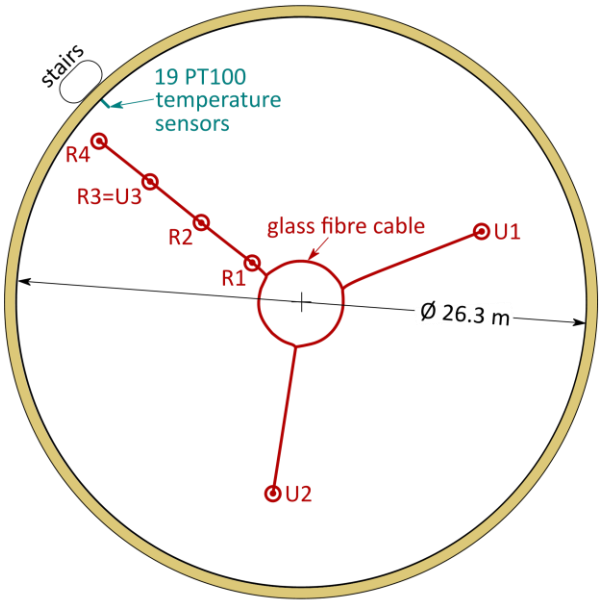

parameter	value	dim.
diameter	26.3	m
height	40	m
max. volume flow	900	m^3/h
max. supply temperature	98	°C
min. return temperature	60	°C

Figure 2: Measurement concept of the atmospheric one-zone heat storage tank and main design parameters

of the DTS system. Thus, for cases with no charging or discharging radial homogeneity of the temperature field can be assumed. Therefore, this case is considered as reference case for further investigation.

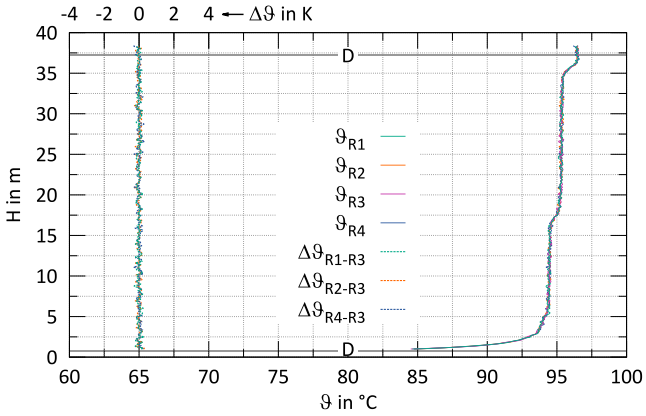

Figure 3: Temperature profile at the four radial positions and Temperature difference to R3 with scale on x2-axis. Reference case, 15 June 2016, 12.00 am

In the measurement period from 04 May to 30 June 2016 the largest radial deviation of 3.8 K occurs at 00.28 am on 31 May between R1 and R3 (dashed lines on the left side of Figure 4). It is located in the lower half of the thermocline at about 31.5 m. The maximum radial deviation is caused by an inversion lasting 1.45 h while a discharging process where water enters the heat storage tank at almost 77 °C with a volume flow of 500 m³/h through the lower diffuser. The surrounding fluid has a temperature of 67.5 °C leading to a buoyancy of the incoming fluid, which is associated with strong convective mixing. Nevertheless, all observed radial temperature differences are smaller than 0.4 K in the cold layer, which extends to a height of 30 m (Figure 4). Thus, the inversion does not affect the radial homogeneity in the cold layer significantly compared to the reference case with radial differences up to 0.3 K (Figure 3).

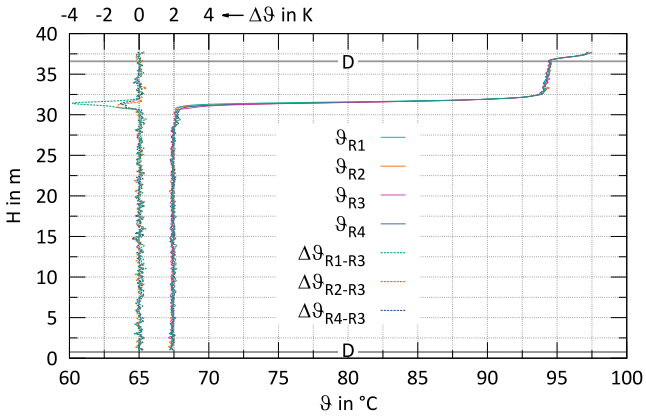

Figure 4: Temperature profile at the four radial positions and Temperature difference to R3 with scale on x2-axis. Reference case, 31 May 2016, 00.28 am

A detailed animated analysis over successive time steps suggests the following thesis for the radial deviations of up to 3.8 K located in the thermocline: Due to its high vertical density gradient the thermocline represents a barrier to the upward convection movement which was caused by the inversion at the lower diffuser. The upward momentum of the convection flow is dissipated by the natural density stratification in the thermocline, bringing it into a slight oscillation. Thus, the temperature profiles in the area of the thermocline seem to be vertically shifted by 0.1 to 0.2 m during this phase. Meanwhile cold water mixes into the thermocline and chills it. The warm storage layer above the thermocline, however, remains unaffected. By the end of the inversion the temperature profiles regain congruence within a few minutes. However, inversions up to this magnitude represent a rare operating case and the described case occurred during commissioning phase of the heat storage tank.

Finally, the radial homogeneity of the temperature field for a typical charging phase of 12 h without pronounced inversions shall be discussed. The maximum volume flow is 850 m³/h. Again, the temperature difference between R1 and R3 is evaluated. Evaluating all temperature differences between R1 and R3 over the total height of the measuring section 466,727 individual temperature differences can be determined from 660 1-minute averages. The obtained dataset is characterized by a very good radial homogeneity of the temperature field. Only 1 % of the temperature differences are outside the range of ±0.3 K with a maximum deviation of 0.8 K.

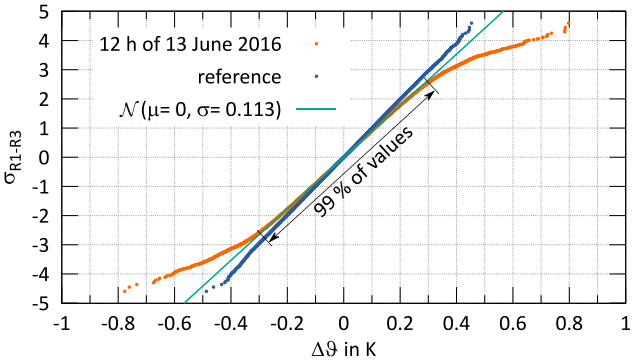

Figure 5: Normal probability plot of temperature differences R1 to R3 while a period of maximum charge flow, 13 June 2016 from 12.00 am to 12.00 pm; reference case, 13 h of 15 June 2016 while a period of no volume flow

A more detailed analysis of this distribution is possible by a comparative analysis with the reference case presented in the normal probability plot (Figure 5). Here, normally distributed data is arranged along a line of constant slope. For the reference case the dataset of 466,621 points approximates the normal distribution very good (blue in Figure 5). This means that in the reference case the temperature differences in radial direction consist in fact only of random noise of the DTS-measurement. The measured 466,727 temperature differences during the charging phase are depicted in orange in Figure 5. Their standard deviation had been calculated to 0.113 K. The straight green line in Figure 5 would result from a perfect normal distribution

with just this standard deviation of 0.113 K. In the top and bottom regions, the orange data deviates from the linear curve.

Therefore, the temperature differences greater than ±0.3 K cannot be explained by the random noise of the DTS-system, which is approximately normally distributed. They must be caused by the temperature field of the heat storage tank. By analyzing the supplementary operating data it was found that the largest radial deviations (>0.6 K) in Figure 5, as already described with reference to Figure 4, are correlated to short term temperature inversions at the upper diffuser. In the period shown for Figure 5, however, the inversions are less pronounced than the inversion of over 9 K, which caused a radial temperature difference of 3.8 K in Figure 4. The inversions during the period shown in Figure 5 reach 2 to 3 K for the temperature difference between the water entering the heat storage tank through the upper diffuser and the surrounding water of the warm layer. Short-term perturbations of the density stratification associated with this 2 to 3 K temperature deviations at the diffuser are thus sufficient to cause very small deviations in the otherwise radially homogeneous heat storage tank.

3. ATMOSPHERIC TWO-ZONE HEAT STORAGE TANKS

3.1 General physics and operating mode

The atmospheric two-zone heat storage tank is also based on HEDBÄCK and is shown as an example in Figure 6 (not to scale). It has the same design features as the one-zone atmospheric heat storage tank, but is divided into two zones by an insulated, dome-shaped intermediate floor. The intermediate floor can be considered dimensionally stable.

The two storage zones each have two radial diffusers for charging and discharging. Moreover the two-zone heat storage tank features a vertical compensation pipe. This is an open ended pipe which serves as a hydraulic connection between the upper and lower storage zone. The length of the pipe and the amount of additional openings depend on constructive and functional requirements. The permanent exchange of fluid between the two storage zones is important for two reasons:

The density changes occurring in the upper storage zone through charging and discharging have a direct effect on the filling level due to approximately constant fluid mass

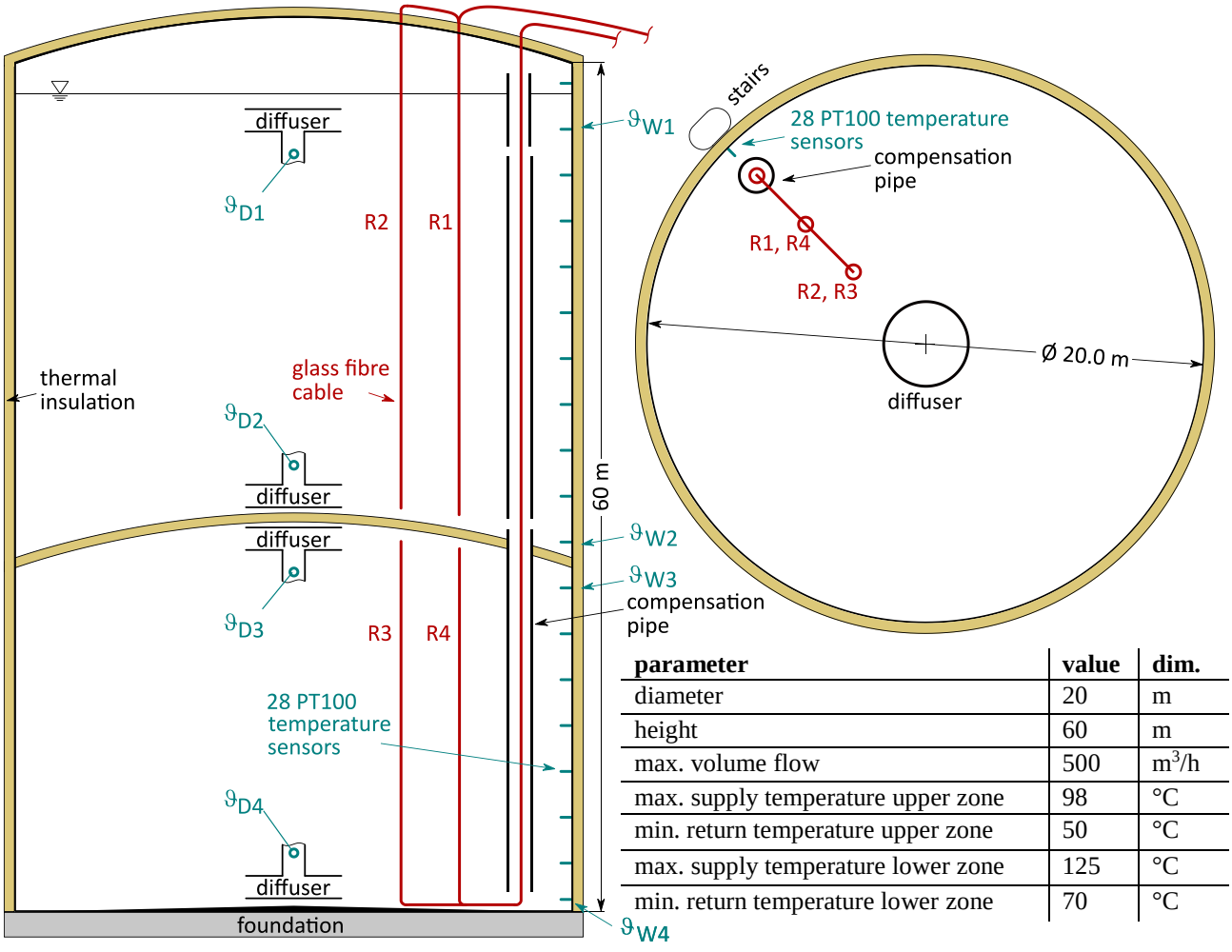

parameter	value	dim.
diameter	20	m
height	60	m
max. volume flow	500	m^3/h
max. supply temperature upper zone	98	°C
min. return temperature upper zone	50	°C
max. supply temperature lower zone	125	°C
min. return temperature lower zone	70	°C

Figure 6: Atmospheric two-zone heat storage tank. Sketch, measurement concept and main design parameters

in the storage tank. In the lower storage zone, however, the volume is constant due to the fixed position of the intermediate floor. Since there is no further expansion tank available for the heat storage tank, the density changes occurring during charging and discharging of the lower storage zone must be compensated for by a mass flow via the compensation pipe.

Moreover, it acts as a safeguard against underpressure or overpressure in the lower zone (e. g. as a result of operating errors).

On the other hand, the exchange of fluid between the two storage zones may encourage undesirable effects:

The compensating pipe primarily conveys fluid from one storage zone to the other, or as a side effect within a storage zone itself in case of additional openings in the compensating pipe. Thus a flow in the immediate vicinity of the respective opening is induced as fluid leaves the compensation pipe. Furthermore, this fluid usually has not the same temperature as the surrounding fluid when entering the respective layer within a storage zone. Due to the necessarily occurring convective mixing, the thermal stratification existing within a storage zone can be influenced negatively.

Nevertheless, the hydraulic coupling of both storage zones has an important effect, which is an essential feature of the two-zone heat storage tank:

The pressure level in the upper region of the lower storage zone below the intermediate floor is sufficiently high to store water at temperatures above 100 °C. Currently, temperature levels of up to 130 °C are in use. These temperature levels do not mark the physical limits but meet the local applicable safety measures.

Thereby, the volume-specific heat capacity of the two-zone heat storage tank is higher compared to a single-zone heat storage tank of the same size. Thus, the higher total investment costs can be super-compensated with respect to the amount of stored energy.

The constructive design of the two-zone atmospheric heat storage tank is not akin to that of the pressurized heat storage tank, since

- the maximum pressure level reached is not higher than with a single-zone atmospheric heat storage tank of the same height
- the heat storage tank is operated as a displacement heat storage tank at atmospheric conditions, and
- the intermediate floor experiences only a small pressure difference.

For atmospheric two-zone heat storage tanks there are two application possibilities: If heat is to be provided at two different temperature levels, both the lower and the upper storage zone can be used actively for heat storage. Alternatively, the sole active operation of the lower storage zone is possible. In this case the upper storage zone serves as pressure load and may be used as water reservoir, for example.

3.2 Measurement concept

The measurement setup features vertical temperature profiles at two radial positions both in the upper and lower zone of the heat storage tank as well as in the compensation pipe (Figure 6). The vertical temperature profiles at positions R1 in the upper zone and R4 in the lower zone had been captured at the same radial distance from the diffusers. The same applies to the vertical profiles at R2 and R3. DTS-measurements had been carried out alternating for the upper and lower zone with an average time of 10 s each. Subsequently, time averaging had been applied to groups of three datasets so that a measuring time of 30 s for one cable represents an average value for one minute of physical time.

Supplementary operating data is available in 1-minute resolution for volume flow of the upper and lower zone, pressure at the bottom, supply and return temperatures for both the upper and lower zone and 28 vertically aligned PT100 sensors.

3.3 Nominal operation, interaction between the upper and lower zone

To show the nominal operation of the two-zone heat storage tank the data record of one measurement day, 26 March 2015, had been chosen according to the following requirements:

- pronounced thermal stratification both in the upper and lower zone as well
- charging or discharging at moderate volume flows both in the upper and lower zone with visible changing of the state of charge
- visible influence of the thermal stratification by the interaction of the two zones through the compensation pipe.

Figure 7 depicts subset operating data including the supply and return temperatures ϑ_D1-ϑ_D4 which had been captured in the corresponding supply and return line. Furthermore, the PT100 temperatures ϑ_W1-ϑ_W4 at the highest and at the lowest position within the two zones of the heat storage tank are shown. The corresponding volume flow is only measured for the return line connecting pipe for each zone. At the other diffuser almost the same inverse mass flow is assumed. Here, positive volume flows indicate charging and negative volume flows indicate discharging.

The lower zone experiences discharging from 00.00 am to 08.00 am with a volume flow of less than 50 m^3/h (or 10 % of nominal volume flow), supply and return temperatures are 118 °C and 73 °C.

Subsequently, there is a phase with zero volume flow followed by discharging in two phases beginning at 00.30 pm, supply (ϑ_D3) and return (ϑ_D4) temperatures are 125 °C and 73 °C.

The upper zone is charged with a volume flow of 50 m^3/h (or 10 % of nominal volume flow) throughout the day. Supply (ϑ_D1) and return (ϑ_D2) temperatures remain constant at 95 °C and 52 °C.

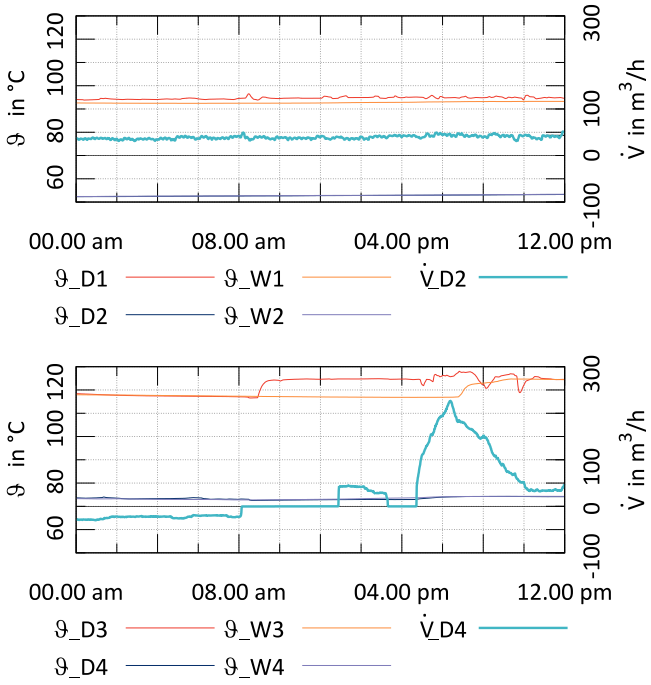

Figure 7: Operating data for upper (top) and lower zone (bottom), 26 March 2015

The evolution of the vertical temperature profile in time generated by post-processing the DTS-measurements is depicted in Figure 8 by height-to-temperature plots. There is one graph for each the upper and lower zone including the temperature profiles every four hours at the radial positions R1 and R4 respectively. The inner temperature profiles R2 and R3 had not been taken into account as they serve to investigate radial homogeneity of the temperature field. However, radial effects are supposed to be small and not to determine main characteristics of the temperature field.

Additional marks in the graphs indicate the positions of the radial diffusers ("D"). In case of the upper diffuser of the upper zone the range where the diffuser can move is marked. The letter "B" marks the position of the intermediate floor within the graph of the upper zone.

General description of the temperature field:

Good thermal stratification can be observed both in the upper and lower zone. Since the pressure level in the lower zone is higher than in the upper zone the temperature level of the lower zone can exceed that of the upper zone. This results in a remarkable aspect of the two-zone heat storage tank: The highest temperature can be found under the intermediate floor at the top of the lower zone and the lowest temperature can be found directly above the intermediate floor at the bottom of the upper zone.

Furthermore, there is obviously more than one thermocline in the lower zone which is the regular case and occurs due to fluctuating supply and return temperatures. However, in the presented case no further fluctuations occur which facilitates the discussion of the evolution of the temperature profiles in time for the two zones.

The same applies to the upper zone. Here, only one thermocline is pronounced whereas the other ones are only implied. In addition for the upper zone several influences on the shape of the temperature profile have to be discussed.

Moreover, the vertical temperature gradient within a pronounced thermocline is higher for the lower zone than for the upper zone.

Evolution of the temperature field in the lower zone:

The temperature profile is shifted vertically while charging and discharging. Between 00.00 am and 08.00 am it moves slightly upwards due to discharging. At 12.00 am the state of charge of the lower zone is identical to 04.00 am as the temperature profile has reached the same position. From this point on the two cycles of charging cause the temperature profile to move downwards. The covered distance between 04.00 pm and 08.00 pm is especially high due to the high volume flow. In addition a third thermocline from 117 °C to 127 °C is formed by the increased level of supply temperature.

During the whole process the shape of the temperature profile remains nearly the same for the thermoclines and the temperature levels at H = 2…4 m and H = 11…17 m. In the upper region above the upper thermocline a slight lowering of the temperature level of approximately 1.5 K can be observed.

Convective mixing is not considered to be the reason for this effect because there is no source of cold fluid entering the lower zone in this region. Heat losses through the surface are not dominating here because they would influence the entire temperature profile. Hence, the lowering of the temperature level in the upper region must be caused by thermal conduction through the intermediate floor. Underneath the intermediate floor the water is cooling down and mixes with fluid of the upper layer, as described in (Huhn, 2007). Subsequently, the upper layer is chilled evenly.

The minimum temperature level is reached at 12.00 am. Afterwards the charging processes combined with an increased supply temperature form a layer with fluid at a higher temperature and a third thermocline which is already implied by the temperature profile at 04.00 pm. The influence of thermal conduction on the temperature level cannot be discussed for the time after 12.00 am as the thermocline at 04.00 pm is not fully developed and the supply temperature is not stable. But the temperature profile at 12.00 pm implies that again the warm layer is cooling down.

The temperature profiles show that the influence of thermal conduction can be proven by the DTS-measurements. This effect could not be detected by the conventional operating data since the shape of the temperature profile is not resolved sufficiently. The modelling of thermal conduction through the intermediate floor is not presented in this paper and is considered as future work.

Evolution of the temperature field in the upper zone:

Figure 8 shows that constant charging of the upper zone is shifting the temperature profile downwards. As the volume flow remains nearly constant the displacement speed is also nearly constant which can be estimated regarding the distance covered by the thermocline at 49 m starting at 00.00 am. The vertical temperature gradient within the thermocline is not influenced. Obviously, the thermocline at about 58 m does not get affected by the charging process. That is because this region marks the transition from the fluid to the vapour space. This is a region above the water level where steam gets induced to keep an approximately constant temperature.

Contrarily to the lower zone the shape of the temperature profile changes more considerably. The following aspects can be observed as marked in Figure 8:

a) The thermal stratification in the region from 52 m to 57 m gets more pronounced during the entire day.

b) At its lower end the thermocline gets blurred meaning that the transition to the temperature level of 54 °C smoothens.

c) The temperature level from 27.5 m to 36 m increases. As a result, the thermocline at 35 m disappears.

Knowing that the compensation pipe features two additional openings, one in proximity of the lowest vertical position of the upper diffuser and one at the bottom of the upper zone, there are two possible influences on the temperature profile in region a):

- Flow leaving the upper diffuser at supply temperature
- Flow leaving the compensating pipe through the upper opening

The first point is likely to influence the temperature profile in the upper layer within region a) since the flow leaving the upper diffuser should form a layer of approximately the same temperature level as the supply temperature.

The lower layer within region a) is outside the sphere of influence of the upper diffuser and must be caused therefore by the flow leaving the compensation pipe. The measurement data shows that the temperature level slightly decreases while the layer gets more pronounced.

Regarding the discharging process in the lower zone from 04.00 pm the fluid originating from the bottom of the lower zone enters the compensation pipe at a temperature of about 74 °C. Since the compensation pipe features a second opening at the bottom of the upper zone permanent exchange between fluid in the compensation pipe and the heat storage tank is possible. For this reason, the temperature level within the compensation pipe is shifted to about 62 °C as fluid is transferred to the upper opening. This chilled fluid enters the upper zone and mixes with the surrounding fluid. Subsequently, a layer of about 87 °C is formed.

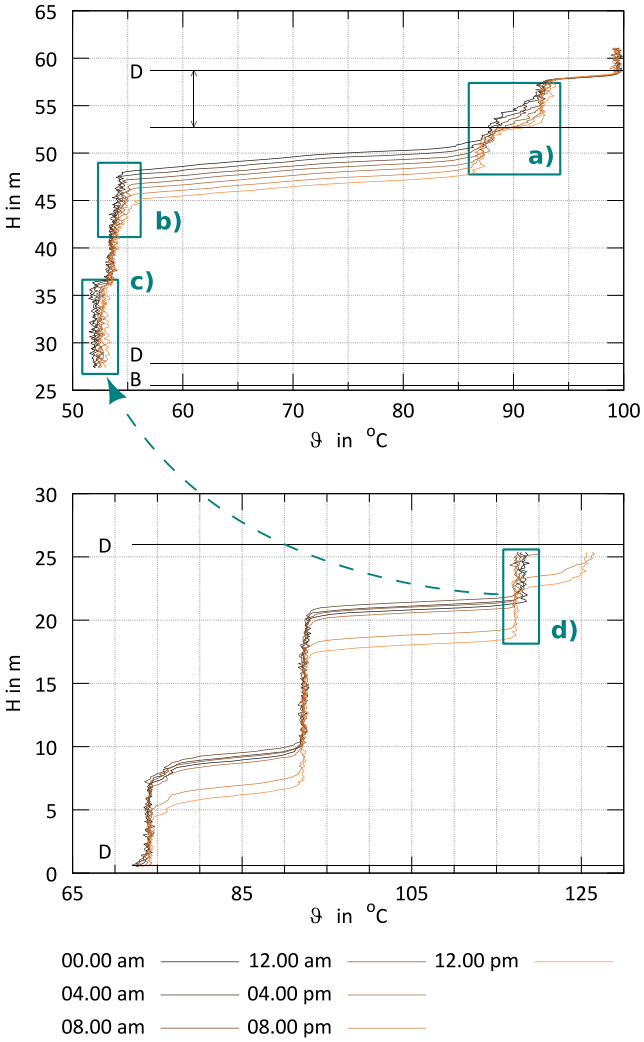

Figure 8: Evolution of temperature profile for the upper (top) and lower (bottom) zone, 26 March 2015

Besides, a small amount of fluid leaving the compensation pipe may also fall through the thermocline and influence the temperature profile in region b). This process could be observed by animated visualization of the DTS-measurements including the temperature profile within the compensation pipe, which is not presented in this paper. The volume of fluid transferred through the compensation pipe for the discharging process of the lower zone from 04.00 pm to 12.00 pm could be estimated to 32 m^3 which is about 0.4 % of the total volume of the lower zone. Nevertheless, this small amount of fluid is able to cause the changes in the temperature profile in the lower layer of region a) which could be confirmed by an energy balance.

For region c) there are four possible influences:

- Flow leaving the lower diffuser at return temperature
- Thermal conduction within the upper zone
- Thermal conduction through the intermediate floor
- Flow leaving the compensation pipe

As there is no fluid leaving the lower diffuser, the first point is deniable. Thermal conduction within the upper zone requires a sufficiently high temperature gradient but is unlikely to act over distances of several metres. However, thermal conduction through the intermediate floor must be taken into account since heat losses in the upper layer of the lower zone had been observed. The heat transfer through the intermediate floor is therefore indicated by a green arrow. Finally, a possible influence might be fluid originating from the bottom of the lower zone and leaving the compensation pipe through the lower opening at the bottom of the upper zone. It may rise up and mix with fluid of the cold layer of the upper zone.

4. FUTURE WORK

One-Zone heat storage tanks

- Evaluate further measuring periods
- Proof of circumferential symmetry
- Creating a simple 1 D model that comprises the main effects on the vertical temperature profile

Two-Zone heat storage tanks

- Proof of radial (and circumferential) homogeneity
- Design of a universal assessment criteria for thermal stratification
- Quantifying thermal losses towards the boundaries and within the heat storage tank, i.e. thermal conduction through the intermediate floor
- Characterizing the flow within the compensation pipe

4. CONCLUSIONS

Large atmospheric heat storage tanks offer a technically approved and cost efficient way to store energy at the temperature level of district heating systems. The DTS-measurement system was found to be an appropriate mean to investigate this type of heat storage tanks in detail.

One-Zone heat storage tanks

In the measuring period of two months, the heat storage tank shows a pronounced radial homogeneity. Only temperature inversions due to warmer fluid leaving the lower or colder fluid leaving the upper diffuser cause radial temperature deviations up to a few Kelvin. These deviations quickly fade away with the end of inversion. The actual thermal stratification of the heat storage tank is hardly affected.

Two-Zone heat storage tanks

The measurement data shows a prove-of-concept for the two-zone heat storage tank design. In this case both the upper and lower zone are used actively to store heat at different temperature levels each. Despite detected inner thermal losses good thermal stratification in both zones can be observed. Besides thermal conduction within the storage medium of a single zone thermal conduction through the intermediate floor and the flow through the compensation pipe are assumed as main influences on inner thermal losses. The latter is a direct consequence of the upper zone serving as pressure maintenance of the lower zone. Hence, to a certain degree an influence on the thermal stratification is expected and unavoidable.

ACKNOWLEDGEMENT

This research project was founded by German Bundesministerium für Wirtschaft und Energie (FKZ 03ET1322A).

REFERENCES

Smolen J. J. and van der Spek A. (2003) *Distributed Temperature Sensing – A DTS Primer for Oil & Gas Production*, Shell International Exploration and Production B. V., The Hague, The Netherlands.

Rühling K. et. al. (2016) *Erhaltung der Marktfähigkeit von KWK Anlagen mittels Einbindung von Umweltenergie*, Abschlussbericht Forschungsvorhaben – FKZ 0327831 (BMWi). AGFW-Projektgesellschaft für Rationalisierung, Information und Standardisierung mbH, ISBN: 3-89999-057-9

Herwig A. and Rühling K. (2014) Fibre-Optic distributed temperature sensing of large hot water storage tanks. *14th International Symposium on District Heating and Cooling*, 7-9 September, Stockholm, Sweden.

Huhn R. (2007) *Beitrag zur thermodynamischen Analyse und Bewertung von Wasserwärmespeichern in Energieumwandlungsketten*, PhD Thesis, Technische Universität Dresden.